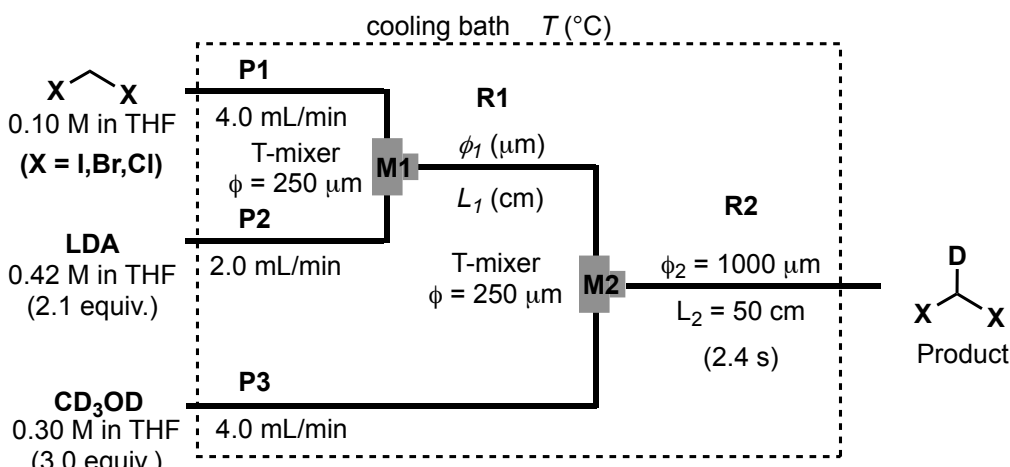


Electronic supporting information (ESI)

General information

GC analyses were carried out on a gas chromatograph (column, Rtx-200; 0.25 mm x 30 m) equipped with a mass selective detector operating at 70 eV (EI). GC/MS data were acquired on a GCMS-QP2020 NX (EI, 70 eV, carrier gas: He). Dry tetrahydrofuran and hexane were purchased from Kanto Chemical Co., Inc. or Fujifilm Wako Pure Chemicals and used without further purification. Stainless steel (SUS304) T-shaped micromixers with inner diameters of 250 μm were manufactured by Sanko Seiki Co., Inc. Stainless steel (SUS316) microtube reactors with inner diameter of 1000 μm purchased from GL Sciences were used unless otherwise stated. The micromixers and microtube reactors were connected with stainless steel fittings (GL Sciences, 1/16 OUW). The flow microreactor system was immersed in a cryogenic mixture bath with dry ice and acetone to control the temperature. Solutions were continuously introduced to the flow microreactor system using syringe pumps (Harvard PHD2000), equipped with gastight syringes purchased from SGE. All reactions were carried out under an atmosphere of argon. Lithium diisopropylamide (LDA) [1.09 M in hexane/THF] was purchased from Kanto Chemical Co., Inc. Exposure of diiodomethane to light should be minimized during all manipulations.

General Procedure for lithiation of dihalomethane followed by the quench with methanol-*d*₄ using a flow microreactor system.



A flow microreactor system consisting of two T-shaped micromixers (**M1** and **M2**), two microtube reactors (**R1** and **R2**), and three tube precooling units (**P1**, **P2** and **P3** (inner diameter $\phi = 1000 \mu\text{m}$, length $L = 100 \text{ cm}$)) was used. The flow microreactor system was dipped in a cooling bath (T °C). A solution of dihalomethane (diiodomethane (**1**), bromiodomethane (**2**), chloroiodomethane (**3**), dibromomethane (**4**), bromochloromethane (**5**), dichloromethane (**6**)) (0.10 M in THF) (flow rate: 4.0 mL/min) and a solution of lithium diisopropylamide (LDA) (0.42 M in THF) (flow rate: 2.0 mL/min) were introduced to **M1** ($\phi = 250 \mu\text{m}$) by syringe pumps. The resulting solution was passed through **R1** and was mixed with a solution of methanol-*d*₄ (0.30 M in THF) (flow rate: 4.0 mL/min) in **M2** ($\phi = 250 \mu\text{m}$). The resulting solution was passed through **R2** ($\phi = 1000 \mu\text{m}$, $L = 50 \text{ cm}$ ($t^{\text{R}2} = 2.4 \text{ s}$)). After a steady state was reached, the outgoing solution was collected for 20 seconds in a vessel containing 4 mL of *sat. aq.* NH_4Cl . The yield of monodeuterated dihalomethane (**1-6-monD**) was determined by GC/MS analysis using dodecane as an internal standard. The results obtained by changing the residence time and the temperature are summarized in Table S3.

Yield and Deuteration estimation by GC/MS analysis

Organic layer was analyzed by gas chromatography mass spectrometry. Recovery of diiodomethane (**5**), diiodomethane-*d*₁ (**6**), and diiodometahene-*d*₂ (**7**) were determined by GC analysis ('R 3.69 min) (initial oven temperature, 50 °C (5 min); temperature increase rate, 10 °C/min (15 min); final temperature, 200 °C) using an internal standard (dodecane). Ratio of **5**, **6**, and **7** were determined by GC/MS(EI) analysis considering isotopic distribution of mass peaks (for example, ratio of **6** was **6**/**(5 + 6 + 7)**). Yield was calculated as follows: Yield = (recovery (%)) x (ratio of **Product** in **5**, **6**, and **7** (%)). The results are summarized in Table S1.

Table S1. Lithiation of dichloromethane (**1a**), dibromomethane (**1b**), diiodomethane (**1c**), chloroiodomethane (**1d**), and bromoiodomethane (**1e**) with LDA followed by trapping with methanol-*d*₄ using a flow microreactor system.

Starting Material	Temperature [°C]	L ₁ [cm]	ϕ ₁ [μm]	t ^{R1} [s]	Recovery [%]	Ratio of monoD [%]	Yield of monoD [%]
1a	0	3.5	1000	0.27	81	88	71
	0	12.5	1000	0.98	73	89	65
	0	50	1000	3.92	65	91	59
	0	100	1000	7.85	42	89	37
	0	200	1000	15.7	27	87	23
	-20	3.5	500	0.069	99	46	46
	-20	3.5	1000	0.27	99	86	85
	-20	12.5	1000	0.98	99	88	87
	-20	50	1000	3.92	99	88	87
	-20	100	1000	7.85	99	87	86
	-20	200	1000	15.7	87	85	74
	-40	3.5	500	0.069	99	29	29
	-40	3.5	1000	0.27	99	53	52
	-40	12.5	1000	0.98	99	88	87
	-40	50	1000	3.92	99	88	87
	-40	100	1000	7.85	99	88	87
	-40	200	1000	15.7	99	86	85
	-60	3.5	500	0.069	99	24	24
	-60	3.5	1000	0.27	99	36	36
	-60	12.5	1000	0.98	99	60	59
	-60	50	1000	3.92	99	83	82
	-60	100	1000	7.85	99	84	83
	-60	200	1000	15.7	99	85	84
	-78	3.5	500	0.069	99	21	21
	-78	3.5	1000	0.27	99	31	31
	-78	12.5	1000	0.98	99	31	31
	-78	50	1000	3.92	99	63	62
	-78	100	1000	7.85	99	64	63
	-78	200	1000	15.7	99	64	63

Starting Material	Temperature [°C]	L ₁ [cm]	ϕ ₁ [μm]	t ^{R1} [s]	Recovery [%]	Ratio of monoD [%]	Yield of monoD [%]
1b	0	3.5	1000	0.27	67	89	60
	0	12.5	1000	0.98	53	89	47
	0	50	1000	3.92	20	91	18
	0	100	1000	7.85	8	93	7
	0	200	1000	15.7	6	91	5
	-20	3.5	500	0.069	99	84	83

-20	3.5	1000	0.27	99	87	86
-20	12.5	1000	0.98	99	89	88
-20	50	1000	3.92	75	89	67
-20	100	1000	7.85	60	91	55
-20	200	1000	15.7	47	90	42
-40	3.5	500	0.069	99	60	59
-40	3.5	1000	0.27	99	86	85
-40	12.5	1000	0.98	99	86	85
-40	50	1000	3.92	99	87	86
-40	100	1000	7.85	91	91	83
-40	200	1000	15.7	83	92	76
-60	3.5	500	0.069	99	48	48
-60	3.5	1000	0.27	99	64	63
-60	12.5	1000	0.98	99	70	69
-60	50	1000	3.92	99	76	75
-60	100	1000	7.85	98	89	87
-60	200	1000	15.7	92	89	82
-78	3.5	500	0.069	99	43	43
-78	3.5	1000	0.27	99	55	54
-78	12.5	1000	0.98	99	55	54
-78	50	1000	3.92	99	58	57
-78	100	1000	7.85	99	66	65
-78	200	1000	15.7	99	67	66

Starting Material	Temperature [°C]	L ₁ [cm]	ϕ ₁ [μm]	t ^{R1} [s]	Recovery [%]	Ratio of monoD [%]	Yield of monoD [%]
1c	0	3.5	500	0.069	66	93	61
	0	3.5	1000	0.27	64	94	60
	0	12.5	1000	0.98	18	96	17
	0	50	1000	3.92	3	53	2
	0	100	1000	7.85	3	30	1
	0	200	1000	15.7	n.d.	n.d.	n.d.
	-20	3.5	500	0.069	99	85	84
	-20	3.5	1000	0.27	86	92	79
	-20	12.5	1000	0.98	71	94	67
	-20	50	1000	3.92	29	95	28
	-20	100	1000	7.85	12	94	11
	-20	200	1000	15.7	6	77	5
	-40	3.5	500	0.069	99	76	75
	-40	3.5	1000	0.27	99	92	92
	-40	12.5	1000	0.98	99	94	94
	-40	50	1000	3.92	66	93	61

-40	100	1000	7.85	57	93	53
-40	200	1000	15.7	31	93	29
-60	3.5	500	0.069	99	40	40
-60	3.5	1000	0.27	99	68	67
-60	12.5	1000	0.98	99	78	77
-60	50	1000	3.92	99	92	91
-60	100	1000	7.85	93	93	86
-60	200	1000	15.7	89	94	84
-78	3.5	500	0.069	99	33	33
-78	3.5	1000	0.27	99	44	44
-78	12.5	1000	0.98	99	48	48
-78	50	1000	3.92	99	79	78
-78	100	1000	7.85	99	84	84
-78	200	1000	15.7	99	91	90

Starting Material	Temperature [°C]	L ₁ [cm]	ϕ ₁ [μm]	t ^{R1} [s]	Recovery [%]	Ratio of monoD [%]	Yield of monoD [%]
1d	0	3.5	1000	0.27	64	80	51
	0	12.5	1000	0.98	17	89	15
	0	50	1000	3.92	1	90	1
	0	100	1000	7.85	n.d.	n.d.	n.d.
	0	200	1000	15.7	n.d.	n.d.	n.d.
	-20	3.5	500	0.069	91	79	72
	-20	3.5	1000	0.27	93	88	82
	-20	12.5	1000	0.98	96	91	87
	-20	50	1000	3.92	48	89	43
	-20	100	1000	7.85	26	90	23
	-20	200	1000	15.7	14	91	13
	-40	3.5	500	0.069	99	48	48
	-40	3.5	1000	0.27	99	87	86
	-40	12.5	1000	0.98	99	89	88
	-40	50	1000	3.92	92	90	83
	-40	100	1000	7.85	73	90	66
	-40	200	1000	15.7	60	90	54
	-60	3.5	500	0.069	99	31	31
	-60	3.5	1000	0.27	99	47	47
	-60	12.5	1000	0.98	99	59	58
	-60	50	1000	3.92	99	85	84
	-60	100	1000	7.85	99	89	88
	-60	200	1000	15.7	99	89	88
	-78	3.5	500	0.069	99	27	27
	-78	3.5	1000	0.27	99	37	37
	-78	12.5	1000	0.98	99	42	42
	-78	50	1000	3.92	99	73	72

	−78	100	1000	7.85	99	77	76
	−78	200	1000	15.7	99	79	78
<hr/>							
Starting Material	Temperature [°C]	L ₁ [cm]	ϕ ₁ [μm]	t ^{R1} [s]	Recovery [%]	Ratio of monoD [%]	Yield of monoD [%]
1e	0	3.5	1000	0.27	68	90	61
	0	12.5	1000	0.98	40	91	36
	0	50	1000	3.92	8	93	7
	0	100	1000	7.85	1	77	1
	0	200	1000	15.7	n.d.	n.d.	n.d.
	−20	3.5	500	0.069	99	88	87
	−20	3.5	1000	0.27	93	89	83
	−20	12.5	1000	0.98	81	90	73
	−20	50	1000	3.92	49	90	44
	−20	100	1000	7.85	29	91	26
	−20	200	1000	15.7	7	92	6
	−40	3.5	500	0.069	99	75	74
	−40	3.5	1000	0.27	99	89	88
	−40	12.5	1000	0.98	99	89	88
	−40	50	1000	3.92	92	90	83
	−40	100	1000	7.85	83	91	76
	−40	200	1000	15.7	73	91	66
	−60	3.5	500	0.069	99	40	40
	−60	3.5	1000	0.27	99	70	69
	−60	12.5	1000	0.98	99	85	84
	−60	50	1000	3.92	99	88	87
	−60	100	1000	7.85	99	90	89
	−60	200	1000	15.7	99	90	89
	−78	3.5	500	0.069	99	33	33
	−78	3.5	1000	0.27	99	35	35
	−78	12.5	1000	0.98	99	57	56
	−78	50	1000	3.92	99	62	61
	−78	100	1000	7.85	99	66	65
	−78	200	1000	15.7	99	80	79

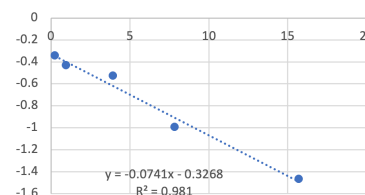
Kinetic evaluation for decomposition rates of dihalomethylolithium intermediates

Kinetic rates are calculated from the plots based on Eq. S1 as depicted below.

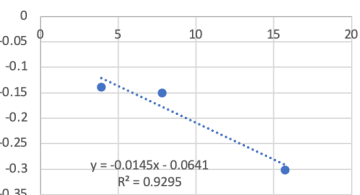
$$\ln[7]/[7_{\max}] = -k \cdot t^{R1} + C \quad \dots \quad (\text{S1})$$

2a (LiCHCl₂)

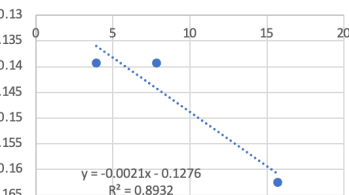
0 °C



-20 °C

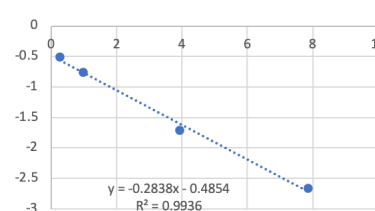


-40 °C

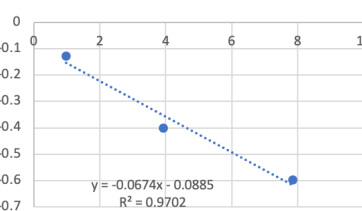


2b (LiCHBr₂)

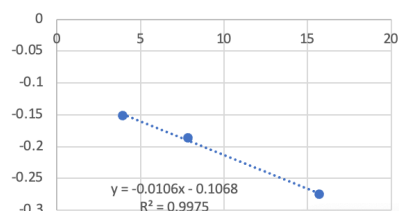
0 °C



-20 °C

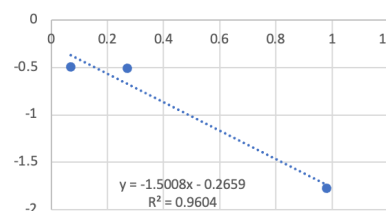


-40 °C

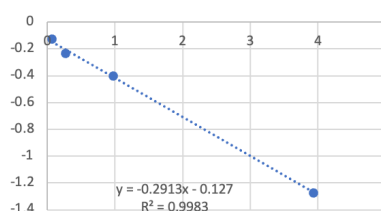


2c (LiCHI₂)

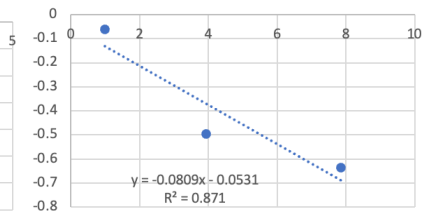
0 °C



-20 °C

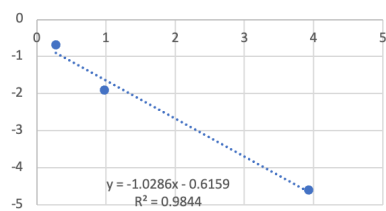


-40 °C

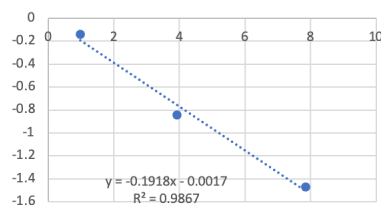


2d (LiCHClI)

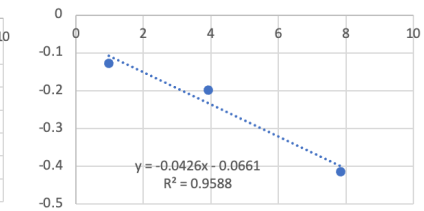
0 °C



-20 °C

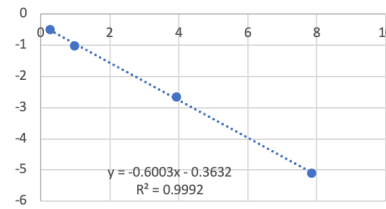


-40 °C

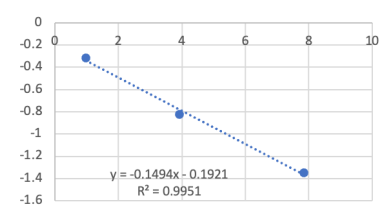


2e (LiCHBrI)

0 °C



-20 °C



-40 °C

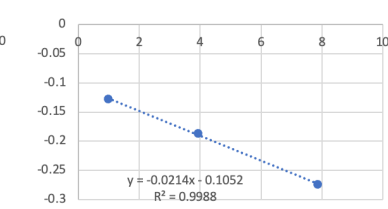


Fig. S1 Kinetic plots corresponding to the decomposition of dihalomethylolithium species. $[7]$ = (concentration of 7a-e), $[7_{\max}]$ = (theoretical maximum concentration of 7a-e) $\sim [1_0]$ = (initial concentration of 1a-e). All plots for 7a-e at 0, -20, -40 °C are drawn in the figures above. Vertical axis: $\ln[7]/[7_{\max}]$, horizontal axis: residence time t^{R1} (s)

Theoretical calculations

Geometries for all compounds have been optimized by the MP2/6-31+G(d) level of theory. Accurate bond energies have been obtained by the CCSD(T)¹ single-point energy calculations with aug-cc-pVDZ² and aug-cc-pVDZ-PP³ basis sets for the normal and iodine atom respectively. All calculations have been carried out with Gaussian16⁴ program. The calculated dissociation energies of dihalomethyl lithium (ΔE_0) are listed with total energy and zero-point energy (ZPE) for each molecule/radical in Table S4.

Table S2. Calculated energies

	total energy [a.u.]	ZPE [a.u.]	ΔE_0 [kcal/mol]
LiCHI-I	-635.71057	0.01608	58.6
LiCHI	-340.83023	0.01306	
I	-294.78387	0.00000	
LiCHBr-Br	-5191.16297	0.01659	65.8
LiCHBr	-2618.55023	0.01296	
Br	-2572.50419	0.00000	
LiCHCl-Cl	-965.40465	0.01768	72.6
LiCHCl	-505.67064	0.01326	
Cl	-459.61390	0.00000	
LiCHBr-I	-2913.46550	0.01644	80.3
LiCHBr	-2618.55023	0.01296	
I	-294.78387	0.00000	
LiCHCl-I	-800.57547	0.01717	73.5
LiCHCl	-505.67064	0.01326	
I	-294.78387	0.00000	

References

1. J. A. Pople, M. Head-Gordon, K. Raghavachari, *J. Chem. Phys.* 1987, **87**, 5968.
2. T. H. Dunning, *J. Chem. Phys.* 1989, **90**, 1007.
3. K. A. Peterson, D. Figgen, M. Dolg, H. Stoll, *J. Chem. Phys.* 2007, **126**, 124101.
4. M. J. Frisch, G. W. Trucks, H. B. Schlegel, G. E. Scuseria, M. A. Robb, J. R. Cheeseman, G. Scalmani, V. Barone, G. A. Petersson, H. Nakatsuji, X. Li, M. Caricato, A. V. Marenich, J. Bloino, B. G. Janesko, R. Gomperts, B. Mennucci, H. P. Hratchian, J. V. Ortiz, A. F. Izmaylov, J. L. Sonnenberg, D. Williams-Young, F. Ding, F. Lipparini, F. Egidi, J. Goings, B. Peng, A. Petrone, T. Henderson, D. Ranasinghe, V. G. Zakrzewski, J. Gao, N. Rega, G. Zheng, W. Liang, M. Hada, M. Ehara, K. Toyota, R. Fukuda, J. Hasegawa, M. Ishida, T. Nakajima, Y. Honda, O. Kitao, H. Nakai, T. Vreven, K. Throssell, J. A. Montgomery, Jr., J. E. Peralta, F. Ogliaro, M. J. Bearpark, J. J. Heyd, E. N. Brothers, K. N. Kudin, V. N. Staroverov, T. A. Keith, R. Kobayashi, J. Normand, K. Raghavachari, A. P. Rendell, J. C. Burant, S. S. Iyengar, J. Tomasi, M. Cossi, J. M. Millam, M. Klene, C. Adamo, R. Cammi, J. W. Ochterski, R. L. Martin, K. Morokuma, O. Farkas, J. B. Foresman, and D. J. Fox, Gaussian, Inc., Wallingford CT, 2016.